Monatshefte für Chemie 132, 1189–1200 (2001)

Monatshefte für Chemie
Chemical Monthly

Effects of HNO_3 Concentration on the Electrochemical Behaviour of Lead

Maher M. EL-Naggar

Chemistry Department, Faculty of Science, Benha University, Benha, Egypt

Summary. The voltammogram of lead in nitric acid shows two well-defined anodic waves during the positive potential sweep. Upon reverse scanning, a wide current plateau followed by a cathodic peak associated with a shoulder at extreme negative potentials is observed. The overall behaviour was found to be quite complicated, and no simple relation between various variables like peak currents, peak potentials, and electrolyte concentrations could be found. The implications of these results with respect to the mechanisms of the electrode reactions are discussed.

Keywords. Lead; Nitric acid; Cyclic voltammetry; Redox reactions.

Introduction

The electrochemical behaviour of Pb in aqueous solutions has been published previously [1–14]. In spite of numerous publications dealing with Pb in HNO_3 of different concentrations [15–20], no work in this field has been done using cyclic voltammetry. Generally, it has been reported that the rate of Pb dissolution in HNO_3 increases with increasing acid concentration up to a certain point; thereafter, the reaction is inhibited [15–17]. Several authors have studied the mechanism of Pb corrosion in HNO_3 [16–20], proposing that at low HNO_3 concentrations the dissolution of Pb takes place according to the autocatalytic mechanism suggested by *Evans* [21]. On the other hand, the inhibition of lead corrosion at high HNO_3 concentrations has been attributed to the formation of a protective lead dioxide surface layer [16, 19]. Great effort has been directed to the understanding of the electrochemistry of lead oxides [22] owing to their importance in electrochemical technology [23].

The present investigation reports the results of a study on the electrochemical behaviour of lead at different HNO_3 concentrations using cyclic voltammetry.

Results and Discussion

General features

Figure 1 presents the cyclic voltammogram of lead electrodes in HNO_3 solutions of different concentrations (1.0–5.0 $mol \cdot dm^{-3}$) between -1.3 and $+3.0$ V *vs.* SCE

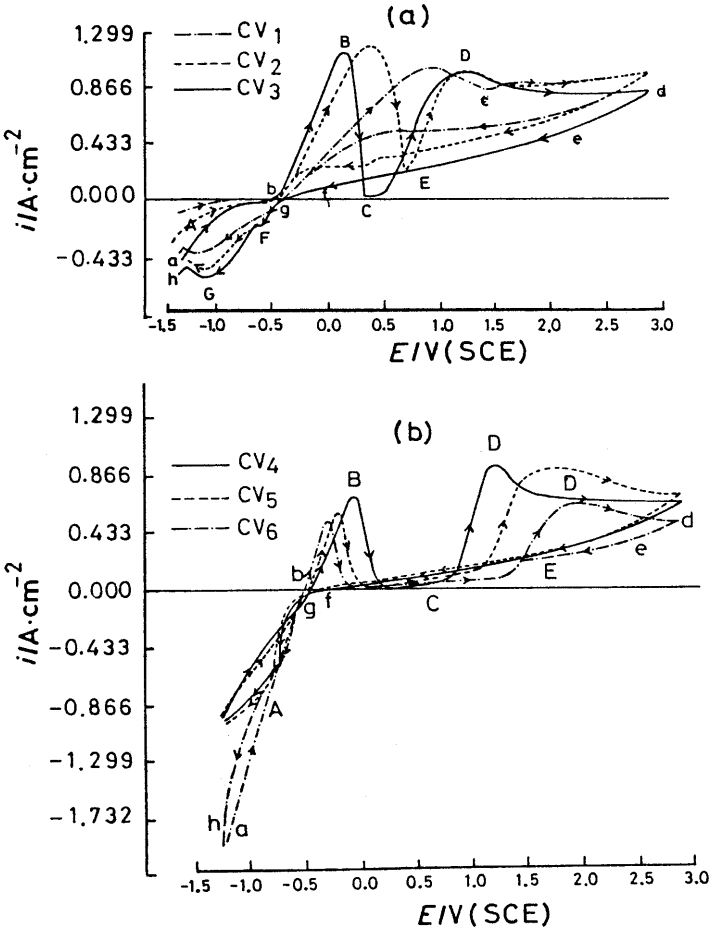

Fig. 1. Cyclic voltammograms of a lead electrode in HNO_3 solutions of different concentrations at a sweep rate of $10\,mV \cdot s^{-1}$ and 25°C; (a) low and moderate HNO_3 concentrations: $1.0\,mol \cdot dm^{-3}$ (CV_1), $2.0\,mol \cdot dm^{-3}$ (CV_2), $3.0\,mol \cdot dm^{-3}$ (CV_3); (b) high HNO_3 concentrations: $4.0\,mol \cdot dm^{-3}$ (CV_4), $4.5\,mol \cdot dm^{-3}$ (CV_5), $5.0\,mol \cdot dm^{-3}$ (CV_6)

at a scan rate of 10 mV/sec and 25°C. All curves show the same general shape: two well-defined anodic waves and one cathodic wave at extremely negative potential. The complete voltammogram is characterized by several features marked by A, B, C, and D on the forward (anodic) half-cycle and by E, F, and G on the backward (cathodic) half-cycle. The main differences between the curves can be attributed to the effect of HNO_3 concentration. Obviously, there are two different accordingly patterns, and the curves can accordingly be divided into two main groups: a) low and moderate HNO_3 concentration ($\leq 3.0\,mol \cdot dm^{-3}$, Fig. 1a) and b) high HNO_3 concentration ($>3.0\,mol \cdot dm^{-3}$, Fig. 1b). In other words, it appears that $3.0\,mol \cdot dm^{-3}$ is in some way a critical acid concentration.

The present detailed discussion refers to the case of $c = 1.0\,mol \cdot dm^{-3}$; the effect of increasing nitric acid concentration will be outlined relative to that reference concentration.

Forward half-cycle

The anodic branch of the voltammogram of a lead electrode in $1.0\,\mathrm{mol}\cdot\mathrm{dm}^{-3}$ HNO_3 (Fig. 1a, CV_1, curve abcd) consists of a starting point (a), an arrest (A), a well-defined first anodic wave (B), a point of contact (c), and finally a well-defined second anodic wave (D). The starting point at (a, -1.30 V) consists of an initial rise in potential leading to a horizontal arrest A at which the current is still cathodic. By analogy with similar studies, region A could either be due to the decay of a cathodic process, or to the reduction of impurities as well as to charging of the electrode double layer. This residual current will flow until the potential becomes sufficiently high to effect the beginning of the main oxidation process (b, -0.450 V). Beyond point b, the anodic current density rises to a maximum value ($E_{\mathrm{peak}} = 0.875$ V, $i_{\mathrm{peak}} = 0.99\,\mathrm{A}\cdot\mathrm{cm}^{-2}$) and then descends, thus forming the first anodic wave B which ends at point c. This first anodic wave B could be attributed to the first oxidation step producing Pb(II) ions and forming Pb(II) species (salt or oxide). Along this region, the formation of a white layer is observed on the electrode surface. This film could be the result of the formation of lead nitrate and/or lead oxide depending on the experimental conditions. Judging from the value of the current density at point c, it can be concluded that this surface layer is too porous to impart passivation. However, it will add resistance polarization and thus affect the rate of dissolution.

At point c, the anodic current density starts to rise again (maximum value: $E_{\mathrm{peak}} = 1.594$ V, $i_{\mathrm{peak}} = 0.89\,\mathrm{A}\cdot\mathrm{cm}^{-2}$) and then falls off, developing the second anodic wave (D). The presence of two successive waves (B and D) implies that the anodic process most probably consists of two steps (*i.e.* $\mathrm{Pb(0)} \rightarrow \mathrm{Pb(II)} \rightarrow \mathrm{Pb(IV)}$). In other words, wave D represents further oxidation of the previously formed anodic product (*i.e.* dissolution of Pb(IV) ions with formation of Pb(IV) species). The PbO_2 layer formed anodically on the electrode surface at very high positive potentials could be the result of hydrolysis or oxidation of either lead nitrate and/or lead oxide (for a discussion of the mechanism, see below).

Backward half-cycle

The backward half-cycle of the lead electrode in $1.0\,\mathrm{mol}\cdot\mathrm{dm}^{-3}$ HNO_3 solution (Fig. 1a, CV_1, curve defgh) consists of a starting point d at vertex potential, a decay curve de, a current plateau E, a decay curve fg, a shoulder F, and finally a cathodic peak G at extremely negative potential.

Upon reversing the potential scan at the vertex (point d) the current remains anodic, indicating the continuation of anodic processes. By analogy with similar studies, the capacitive current decays along curve de leading to a current plateau E, which extends over a long potential span. The constancy of the current along plateau E indicates the stability of the previously formed PbO_2; it might also be attributed to the presence of a limiting phenomenon of a surface layer next to the electrode surface. All these phenomena result most probably from resistance polarization originating from the previously formed surface film. Judging from the value of the current density, it cannot be attributed to a passivation phenomenon. It is important to note that the current plateau E decays along curve fg to point g which coincides with point b of the forward scan, thus forming a singularity.

Beyond this unique point, a new cathodic peak G with an associated shoulder F appears at extremely negative potential. This region can most probably be attributed to the cathodic reduction of nitric acid.

In conclusion, the main features of the cyclic voltammogram of lead in $1.0\,\mathrm{mol}\cdot\mathrm{dm}^{-3}$ HNO_3 consist of two consecutive oxidation steps and one cathodic wave with an associated shoulder at extremely negative potential (end of the reverse sweep).

Effect of nitric acid concentration

From the cyclic voltammograms of lead in nitric acid solutions of different concentrations (1.0–$5.0\,\mathrm{mol}\cdot\mathrm{dm}^{-3}$) it can be seen that increasing nitric acid concentration gives essentially similar voltammograms, but affects markedly the peak currents and peak potentials of the waves (Fig. 1). In addition, two important changes of the main features take place: transformation of point c to a plateau C and absence of the cathodic wave above $3.0\,\mathrm{mol}\cdot\mathrm{dm}^{-3}$. In parallel, the stability of the unique joint-point is not changed.

The current arrest A in the forward scan, which appears only in solutions of low and moderate acid concentrations ($\leq 3.0\,\mathrm{mol}\cdot\mathrm{dm}^{-3}$), is transferred to a linear rise in potential in concentrated solutions ($>3.0\,\mathrm{mol}\cdot\mathrm{dm}^{-3}$). The cathodic wave G with its shoulder F decreases gradually until it is finally mutates to a linear potential coinciding with that of the corresponding forward scan.

Regarding the first anodic wave B, its peak potential shifts to a more negative value with increasing HNO_3 concentration; the peak current increases up to $3.0\,\mathrm{mol}\cdot\mathrm{dm}^{-3}$ and then decreases. The potential of the second anodic wave D shifts slightly to more negative values up to $c = 3.0\,\mathrm{mol}\cdot\mathrm{dm}^{-3}$ and then changes to more positive potentials. In parallel, the current density increases and then decreases. It can be clearly seen from Figs. 2 and 3 that no simple relation can be established between peak potentials or peak currents and nitric acid concentration. This indicates that the behaviour of a lead electrode in nitric acid of different concentration is quite complicated. Moreover, the point of contact (c) between the two anodic waves B and D observed in $1.0\,\mathrm{mol}\cdot\mathrm{dm}^{-3}$ HNO_3 is transferred to a current arrest C with a gradual increase in its potential span, reaching 2.125 V at $5.0\,\mathrm{mol}\cdot\mathrm{dm}^{-3}$. It is important to note that the peak potential region is practically unaffected. In other words, the arrest C is mainly the result of a shift of the peak potential of the first wave B to a more negative potential as nitric acid concentration increases. The fact that the acid concentration has a marked effect on the first anodic wave B indicates that the first anodic peak B corresponds to two different partial processes occurring simultaneously (in parallel or stepwise). Depending on the experimental conditions (acid concentration and potential), the first process is predominant at low and moderate HNO_3 concentrations ($\leq 3.0\,\mathrm{mol}\cdot\mathrm{dm}^{-3}$), whereas the other process predominates at high acid concentrations ($>3.0\,\mathrm{mol}\cdot\mathrm{dm}^{-3}$). Within the limits of resolution, the first anodic peak B has therefore to be considered as a composed peak appearing as a single wave.

A comparison between the area (integrated charges Q) under the first wave B and that under wave D give a useful criterion for the detection of soluble reaction products. At low and moderate nitric acid concentrations ($\leq 3.0\,\mathrm{mol}\cdot\mathrm{dm}^{-3}$) the

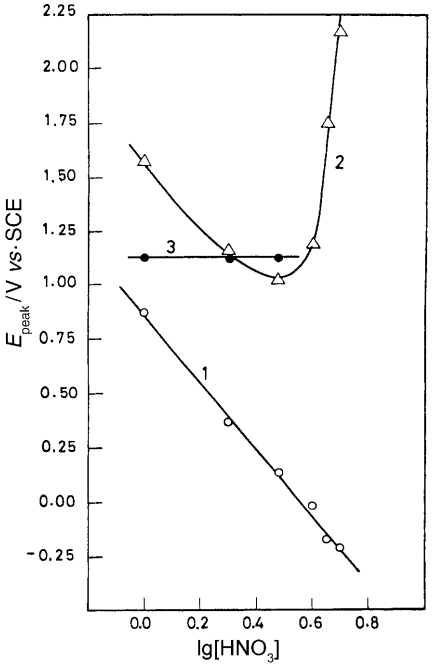

Fig. 2. Dependence of E_{peak} on lg[HNO_3] at a sweep rate of $10\,mV \cdot s^{-1}$; 1: first anodic peak B, 2: second anodic peak D, 3: cathodic peak G

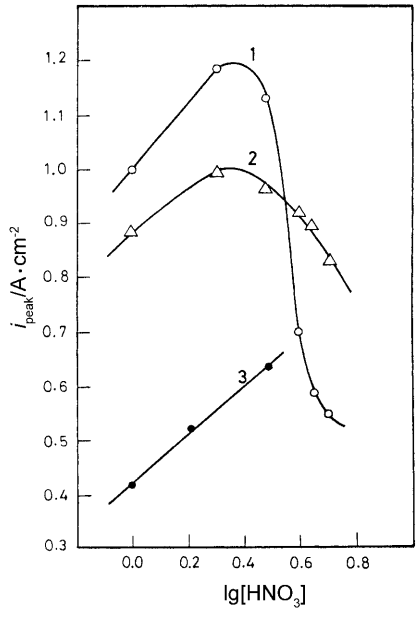

Fig. 3. Dependence of i_{peak} on lg[HNO_3] at a sweep rate of $10\,mV \cdot s^{-1}$; 1: first anodic peak B, 2: second anodic peak D, 3: cathodic peak G

ratio of the integrated charges (Q_B/Q_D) is above 1.0, indicating that a soluble reaction product is formed under the first anodic peak B and diffuses away from the electrode surface; hence, it is not available for further oxidation under the second

anodic wave D. On the other hand, in concentrated nitric acid solutions ($>3.0\,\mathrm{mol}\cdot\mathrm{dm}^{-3}$), Q_B/Q_D is below 1.0, indicating that all corrosion products formed under the first anodic wave B are available for further oxidation under the second anodic wave D. Also, a comparison of the area under wave B at dilute and moderate HNO_3 concentrations with that under wave B in concentrated acid solutions revealed that the ratio $Q_{B(dil)}/Q_{B(conc)}$ is below unity. This indicates that concentrated nitric acid has a strong effect on the nature and, possibly, on the rate of the individual reactions occurring under each wave and leads to the conclusion that the contribution of one component is decreased and the charge involved gives rise to an individual process.

Effect of cycling

Figure 4 represents the effect of cycling on the voltammograms of lead electrodes in 1.0 and $5.0\,\mathrm{mol}\cdot\mathrm{dm}^{-3}$ HNO_3. Three successive cyclings (1, 2, and 3) are shown for each solution. Repeated cycling gives essentially similar voltammograms with remarkable effects on peak currents and peak potentials; the differences can be attributed to the difference in the initial states of the electrode surface. The transformations of the electrode surface material during cycling are related to solubility and diffusion as well as to the rate of growth of $Pb(NO_3)_2$, PbO, and PbO_2 species.

In a $1.0\,\mathrm{mol}\cdot\mathrm{dm}^{-3}$ acid solution (Fig. 4a), the peak current densities increase significantly with the number of cycles due to the activation of the electrode surface by repeated cycles. The peak potentials shift significantly to more positive values, and the waves are more extended, indicating an enhanced reversibility of the process.

At a concentration of $5.0\,\mathrm{mol}\cdot\mathrm{dm}^{-3}$ HNO_3 (Fig. 4b), the effect of cycling is less significant than at $1.0\,\mathrm{mol}\cdot\mathrm{dm}^{-3}$. No difference was observed between the anodic and cathodic branches of the voltammograms, whereas there is a remarkable difference between the currents and potentials of the peaks. For the first anodic wave B, the peak current increases, and the peak potential is shifted to more positive values. For the second anodic wave D, the peak current decreases and then increases again, whereas the peak potential is unaffected by the number of cycles. Furthermore, the cathodic wave region remains practically unaffected. The position of the unique point is practically not affected by the number of cycles.

Effect of voltage excursion

Reverse scan experiments were performed in HNO_3 solutions of different concentrations. The different voltage excursions (CV_1, CV_2, and CV_3) for Pb electrodes in 1.0 and $4.0\,\mathrm{mol}\cdot\mathrm{dm}^{-3}$ HNO_3 are represented in Fig. 5 and show that all cyclic voltammograms start at the same initial potential (-1.3 V). Generally, the effect of voltage excursion gives information about intermediate species formed during the anodic oxidation and helps in exploring the correspondence between the two consecutive waves B and D.

In all solutions the potential scan was reversed immediately after wave B. The expected corresponding cathodic wave is absent, indicating the irreversibility of the

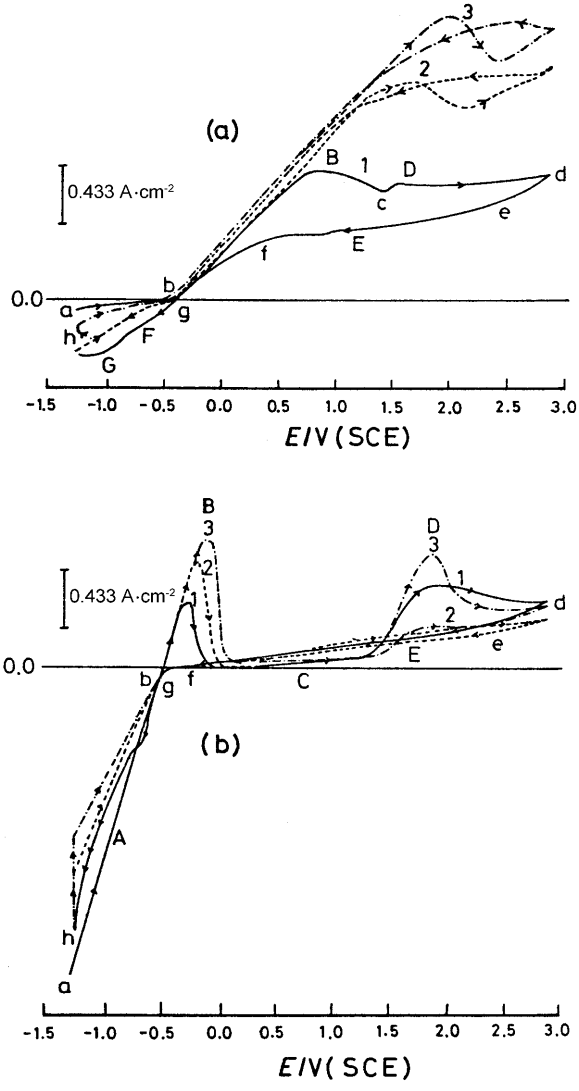

Fig. 4. Three successive sweeps in (a) $1.0\,mol \cdot dm^{-3}$ and (b) $5.0\,mol \cdot dm^{-3}$ HNO_3 solutions at a sweep rate of $10\,mV \cdot s^{-1}$ and 25°C; 1: first sweep, 2: second sweep, 3: third sweep

anodic process under wave B; all corresponding CVs in all solutions are similar. The absence of a corresponding cathodic wave upon scan reversal immediately after the first anodic wave B indicates the presence of a chemical process following the first-electron transfer step. The following chemical reaction is presumably the dissolution of a surface film.

Examination of all voltammograms in all solutions reveals that no cathodic wave is observed in the cathodic branch corresponding to the two anodic waves B and D. Moreover, the most important noticeable effect is that under all experimental conditions the cathodic branch decays rapidly to the same unique point. In other words, voltage excursion has practically no effect on the unique point position; this is due to the solubility and diffusion of all species formed except PbO_2.

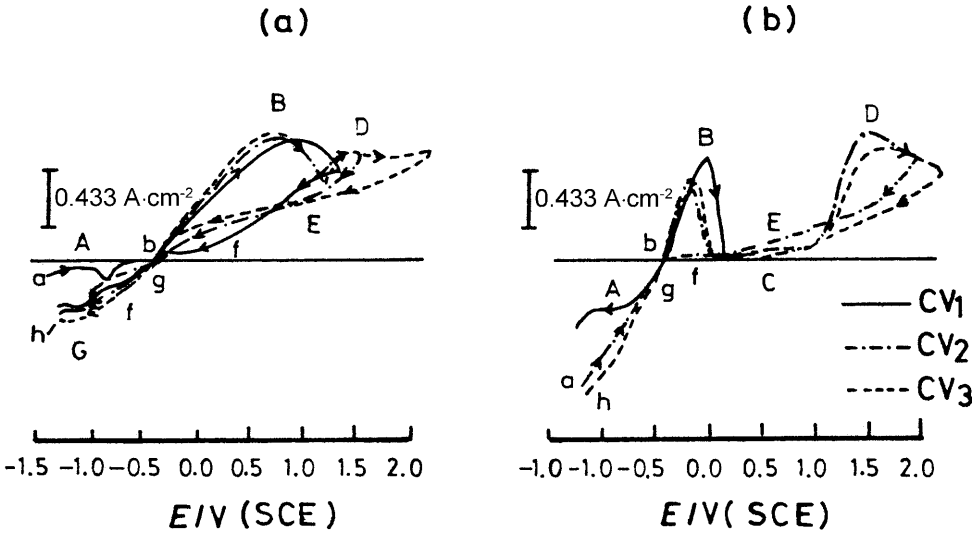

Fig. 5. Cyclic voltammograms of a lead electrode in (a) $1.0\,\mathrm{mol}\cdot\mathrm{dm}^{-3}$ and (b) $4.0\,\mathrm{mol}\cdot\mathrm{dm}^{-3}$ HNO_3 solutions obtained with different reversal potentials ($10\,\mathrm{mV}\cdot\mathrm{s}^{-1}$ scan rate, 25°C)

Mechanisms

The voltammogram of a lead electrode in $1.0\,\mathrm{mol}\cdot\mathrm{dm}^{-3}$ HNO_3 is mainly characterized by two consecutive anodic waves, indicating that the anodic dissolution is of the type Pb(0) → Pb(II) → Pb(IV). It would be expected that under ideal conditions all oxidation products formed under the first anodic wave B should be further oxidized quantitatively under the second anodic wave D. This ideal condition takes place at $3.0\,\mathrm{mol}\cdot\mathrm{dm}^{-3}$ HNO_3. The ratios of the integrated charges (Q_B/Q_D) are >1.0 at HNO_3 concentrations below $3.0\,\mathrm{mol}\cdot\mathrm{dm}^{-3}$ and <1.0 at HNO_3 concentrations above $3.0\,\mathrm{mol}\cdot\mathrm{dm}^{-3}$. Hence, the concentration of HNO_3 has a marked effect on the nature and the rate of the individual reaction occurring at each peak.

The absence of a cathodic counterpart corresponding to the well-recognized anodic wave is a strong evidence of the irreversible nature of all anodic processes. This is further supported by the fact that the width of the anodic waves is larger than that expected for reversible processes and can be additionally verified by the study of voltage excursions.

Wave B could be attributed to the first step of the main anodic dissolution of Pb producing Pb(II) ions and forming Pb(II) species. The observed white layer is caused by the dissolution of the metal until the solubility product is reached, after which precipitation of $Pb(NO_3)_2$ takes place. Precipitation could also be initiated by direct reaction of the anion with the metal; direct oxidation of the metal producing an oxide film is a third possibility. The reactions responsible for the formation of the first anodic layer may be written as follows:

$$Pb + 2HNO_3 = Pb(NO_3)_2 + 2H^+ + 2e^- \quad (1)$$

$$Pb + 2NO_3^- = Pb(NO_3)_2 + 2e^- \quad (2)$$

$$Pb + H_2O = PbO + 2H^+ + 2e^- \quad (3)$$

The first anodic peak B is attributed to both lead nitrate and lead oxide formation. Thus, dissolution and precipitation or direct nucleation and growth are possible mechanisms for the formation of the surface film under anodic peak B. Structure and composition of the complex surface layer depend on the experimental conditions. Lead oxide appears to be the predominant component at dilute and moderate HNO_3 concentrations ($\leq 3.0\,\mathrm{mol}\cdot\mathrm{dm}^{-3}$), whereas lead nitrate is the predominant species in concentrated solutions. Moreover, the present results indicate that this surface film is porous, loosely adherent, soluble in the electrolyte, and provides a certain degree of protection but cannot impart passivation.

Wave D could be attributed to the second step of anodic oxidation and has to be ascribed to the oxidation of species previously formed under wave B. The reactions responsible for the formation of the surface layer may be due to a hydrolysis mechanism as follows:

$$Pb(NO_3)_2 + 2H_2O = \beta\text{-}PbO_2 + 2NO_3^- + 4H^+ + 2e^- \quad (4)$$

$$PbO + H_2O = \alpha\text{-}PbO_2 + 2H^+ + 2e^- \quad (5)$$

$$Pb + 6H_2O = \beta\text{-}PbO_2 + 4H_3O^+ + 4e^- \quad (6)$$

Since the first surface layer formed on the electrode surface is porous, the current density as well as the potential under the pores increase and are appropriate for the formation of PbO_2 within the pores of $Pb(NO_3)_2$ and/or PbO. A layer of PbO_2 is formed at the base of the pores and spread below it (Fig. 6). Once the PbO_2 layer is complete, it throws off the layer of $Pb(NO_3)_2$ and/or PbO, leaving a stable, adherent, non-porous layer of good electronic conductivity.

Region C appears only at moderate and high HNO_3 concentrations as a current plateau extending along an increasing potential span as the acid concentration increases. There is evidence for dissolution and diffusion of part of the surface film under wave B. Since dissolution of the surface film is a chemical process, the current plateau is independent of the potential. Thus, the small current passing along plateau C is believed to represent the amount needed to replenish any destruction of the film by its slow dissolution in the electrolyte.

Region E appears as a current plateau that extends over a wide potential span; it is practically independent of solution concentration and corresponds to a voltage

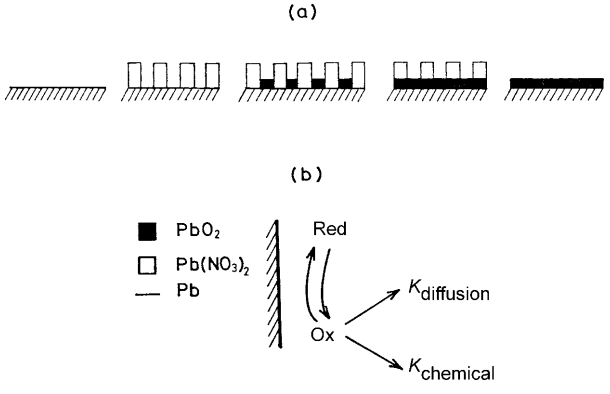

Fig. 6. Schematic illustration of (a) PbO_2 formation mechanism and (b) EC mechanism

drop owing to the resistance of a stable film. It may be distinguished from the other type of polarization (*i.e.* concentration polarization) and might also be attributed to surface morphology changes under the prevailing experimental conditions.

It is important to note that the position of the unique point (*i.e.* the coincidence of points b and g) is practically not affected by the HNO_3 concentration. Over the whole concentration range (1.0–5.0 $mol \cdot dm^{-3}$), the point b of the forward half-cycle corresponds to a bare surface, whereas point g of the backward half-cycle corresponds to the surface covered by PbO_2 film. This corresponds to two different states; yet they have the same function and play the same role. The conclusion that could be drawn from this observation would be that the PbO_2 surface film has a good electric conductance.

At dilute and moderate HNO_3 concentrations ($\leq$3.0 $mol \cdot dm^{-3}$), wave G with its shoulder F is attributed to the reduction of nitric acid on the lead electrode surface according to Eq. (7).

$$HNO_3 + 2H^+ + 2e^- = HNO_2 + H_2O \tag{7}$$

From the experimental results, Eq. (7) proceeds in several steps. It is assumed that the reduction of nitric acid rather than hydrogen evolution would take place primary along shoulder F as follows:

$$H^+ + e^- = H \tag{8}$$

$$H + HNO_3 = NO_2 + H_2O \tag{9}$$

The NO_2 thus formed is assumed to be reduced along the cathodic wave G under formation of HNO_2:

$$NO_2 + e^- = NO_2^- \tag{10}$$

$$NO_2^- + H^+ = HNO_2 \tag{11}$$

This self-stimulating reduction of nitric acid (Eqs. (8)–(11)) is identical to the autocatalytic reaction as proposed by *Evans* [21].

In concentrated HNO_3 (>3.0 $mol \cdot dm^{-3}$), the forward and backward features at extremely negative potentials are transformed into two coinciding straight lines. This indicates that the autocatalytic reduction of nitric acid is not feasible in concentrated solutions. Another interesting point is that lead is not susceptible to passivation in the HNO_3 concentration range studied (1.0–5.0 $mol \cdot dm^{-3}$). In nitric acid solutions, lead is not stable because lead nitrate and lead oxide are soluble corrosion products. On the other hand, lead is stable and forms a protective layer at very high positive potentials due to the formation of PbO_2. Moreover, visual observations of the electrode surface reveal the presence of pits whose number was found to increase with increasing acid concentration. This behaviour gives a strong indication for the formation of a protective surface layer composed of PbO_2 in which pitting corrosion could be initiated by the breakdown of this protective oxide layer. Pitting attack could be related to the presence NO_3^- which is considered as a pitting agent for lead [24].

The above discussion illustrates that two electrochemical processes coupled with chemical reactions are observed. Generally speaking, an 'E_1CE_2' mechanism is recognized by a diminished or lacking reverse peak. The electrochemical and chemical reactions may be reversible and/or irreversible with different degrees

of irreversibility. Further studies are required for quantitative analysis of the electrochemical behaviour of lead in HNO_3 solution.

Conclusions

a) The cyclic voltammograms of Pb electrodes in HNO_3 solutions of different concentrations show two well-defined anodic waves and one cathodic wave with an associated shoulder at extremely negative potential.
b) Lead nitrate and lead oxide are expected to form under the first anodic wave (B), whereas PbO_2 is expected to form under the second anodic wave (D).
c) At low and moderate concentrations of HNO_3 ($\leq 3.0\,mol \cdot dm^{-3}$), a cathodic wave with an associated shoulder appears and is ascribed to the reduction of HNO_3.
d) The reduction of HNO_3 is retarded in concentrated solutions ($>3.0\,mol \cdot dm^{-3}$) due to the formation of a protective layer of PbO_2 at the electrode surface.
e) The mechanism of Pb corrosion in HNO_3 solutions of different concentrations can be discussed in view of an E_1CE_2 mechanism.

Experimental

The working electrode consisted of a bar of pure lead metal (Aldrich, 99.99%) covered by epoxy resin, exposing a disk area of $0.385\,cm^2$. Prior to each experiment, the working electrode was polished with different grades of emery papers, degreased with acetone, washed with running doubly distilled water, and finally dried with filter paper. The electrochemical cell was made from pyrex glass with a side compartment separated from the main chamber by fritted glass to accommodate the platinum counter electrode. The reference electrode was a saturated calomel electrode (SCE) with a *Luggin* capillary probe placed near the surface of the working electrode to minimize the ohmic potential drop through the cell.

HNO_3 solutions ($1.0–5.0\,mol \cdot dm^{-3}$) were prepared from analytical grade reagent (Merck) and doubly distilled water. A Wenking potentioscan (type 73) was used to perform the voltammetric measurements. The cyclic voltamograms were recorded from -1.30 to $+3.0\,V$ and plotted using an X–Y recorder at a scanning rate of $10\,mV \cdot s^{-1}$.

References

[1] Codaro EN, Vilche JR (1997) Electrochim Acta **42**: 549
[2] Nilson RR (1993) J Power Sources **41**: 1
[3] Laitinen T, Monahov B, Salmi K, Sundholm G (1993) Electrochim Acta **36**: 953
[4] Guo Y, Wei Z, Hua S (1997) Electrochim Acta **42**: 979
[5] Pavlov D, Iordanov N (1970) J Electrochem Soc **117**: 1103
[6] Valeriote EML, Gallop LD (1977) J Electrochem Soc **124**: 370
[7] Guo Y (1995) J Electrochem Soc **142**: 3378
[8] Barradas RG, Nadezhdin DS (1984) Can J Chem **62**: 596
[9] Varela FE, Gassa LM, Vilche JR (1993) J Appl Electrochem **25**: 364
[10] Abdul Azim AA, El-Sobki KM (1972) Corros Sci **12**: 207
[11] Birrs VI, Shevalier MT (1987) J Electrochem Soc **134**: 802
[12] Birrs VI, Shevalier MT (1987) J Electrochem Soc **134**: 1595
[13] Abdul Azim AA, Anwar MM (1969) Corros Sci **9**: 245
[14] Khairy EM, Abdul Azim AA, El-Sobki KM (1966) J Electroanal Chem **11**: 282

[15] Smolyaninov IS (1971) Kim Kim Tekhnol **14**: 222
[16] Ravdel AA, Gorelik GN (1975) Vses Khim Ova **10**: 335
[17] Tomashov ND (1967) Theory of Corrosion and Protection of Metals. Macmillan, New York, pp 628–631
[18] Sayed SM, El-Shayeb HA (1986) Surf Coat Technol **29**: 51
[19] Abd El-Aal EE, Abd El-Wanees S, Abd El-Aal A (1992) J Materials Sci **27**: 365
[20] Abd El-Waness S, Abd El-Aal EE, Abd El-Aal A (1991) Bull Soc Chim Fr **128**: 889
[21] Evans UR (1960) The Corrosion and Oxidation of Metals. Edward Arnold, London, p 324
[22] Kuna AT (1979) The Electrochemistry of Lead. Academic Press, London
[23] Feng J, Johnson DJ (1990) J Appl Electrochem **20**: 116
[24] Abd El-Rehim SS, Mohamed NF (1998) Corros Sci **40**: 1883

Received December 14, 2000. Accepted (revised) April 9, 2001